The Classification of Superconductors Using Muon Spin Rotation

A D Hillier and R Cywinski

School of Physics and Astronomy
University of St Andrews
St Andrews
Fife KY16 9SS
Scotland

Abstract

In this paper we explore the role of muon spin rotation (μSR) techniques in the characterisation and classification of superconducting materials. In particular we focus upon the Uemura classification scheme which considers the correlation between the superconducting transition temperature, T_C, and the effective Fermi temperature, T_F, determined from μSR measurements of the penetration depth. Within this scheme strongly correlated "exotic" superconductors, ie high T_C cuprates, heavy fermions, Chevrel phases and the organic superconductors, form a common but distinct group, characterised by a universal scaling of T_C with T_F such that $1/10 > T_C/T_F > 1/100$. For conventional BCS superconductors $1/1000 > T_C/T_F$.

The results of new μSR measurements of the penetration depth in superconducting $Y(Ni_{1-x}Co_x)_2B_2C$ and YB_6 are also presented. In $Y(Ni_{1-x}Co_x)_2B_2C$ the decrease of T_C with increasing Co concentration is linked to a marked decrease in the carrier density from $2.9 \times 10^{28} m^{-3}$ at x=0 to $0.6 \times 10^{28} m^{-3}$ at x=0.1, while the carrier mass enhancement remains almost constant at approximately 10. For YB_6 we find evidence of a modest enhancement of the carrier mass (m^*/m=3), and a relatively low carrier density of $0.24 \times 10^{28} m^{-3}$. These results are discussed within the Uemura classification scheme. It is found that neither $Y(Ni_{1-x}Co_x)_2B_2C$ with $T_C/T_F \approx 1/250$ nor YB_6 with $T_C/T_F \approx 1/340$ can be definitively classified as either "exotic" or "conventional", but instead the compounds display behaviour which interpolates between the two regimes.

1. Introduction

The problem of finding an appropriate classification scheme for the remarkably diverse range of known superconducting materials is a long standing one. Nevertheless the literature abounds with claims of discoveries of "new classes" of superconductors, although the nature of the "class" is rarely defined explicitly. In cases where the structural, electronic or magnetic properties of the new superconductor are particularly unusual it is tempting to accept such claims: heavy fermions, high T_C cuprates, organic superconductors and buckminsterfullerenes are all examples of superconducting materials which superficially have little in common either with each other or with the more conventional superconducting elements and compounds and might therefore be considered as genuinely belonging to different classes. However the underlying uniformity of the superconducting ground state and its general conformity with the predictions of BCS theory continues to unite an extraordinarily disparate group of superconducting materials. Consequently over the last few decades there have been numerous attempts to provide an empirical framework, based upon the fundamental parameters of the superconducting state, within which superconducting materials can be compared and contrasted, thus enabling classes of superconductor to be unambiguously identified. For example, until the early 1980s a correlation between the superconducting transition temperature, T_C, and the Sommerfeld constant, ie the coefficient of the linear electronic specific heat γ, was frequently invoked. A plot of log T_C versus logγ was found to yield an approximately universal curve. However, first the heavy fermion compounds, with enormous γs yet low transition temperatures and then, later, the cuprates with modest γs but remarkably high T_Cs proved to be marked exceptions to this universality, apparently confirming their status as members of new, exotic classes of superconductors.

More recently a rather surprising universal scaling relationship has emerged from systematic transverse field muon spin rotation (μSR) measurements of flux penetration in superconducting systems. Uemura and co-workers [1] were the first to recognise the new scaling relationship, observing that for several different members of the family of high temperature cuprate superconductors an initial increase in carrier doping leads to precisely the same linear increase of T_C with the muon spin depolarisation rate, σ. Deviations from linearity, first appearing as a saturation and then a suppression of T_C, only appear at high levels of doping. Remarkably, several Chevrel phase superconductors were also found to follow the same linear relationship, while bismuthates, fullerenes, organic superconductors and heavy fermion compounds exhibit a similar scaling behaviour [2,3].

The correlation between T_C and σ observed in μSR studies has suggested a new empirical framework for classifying superconducting materials. In this paper we shall briefly review the role played by μSR in establishing this new classification scheme, and discuss the underlying physical phenomena responsible for the observed correlations. We shall also present some of our recent μSR measurements on both YB_6 and the topical superconducting nickel borocarbides, $Y(Ni_{1-x}Co_x)_2B_2C$, and attempt to interpret the results of these measurements within the proposed classification scheme.

2. Determination of the superconducting penetration depth by μSR

Transverse field μSR is a particularly powerful and sensitive microscopic probe of the internal field distribution within the mixed state of Type II superconductors. It offers perhaps the most direct and accurate method of measuring the superconducting penetration depth, whilst also circumventing many of the intrinsic problems associated with, for example, bulk magnetisation measurements. The general principles of μSR have been described in the introductory chapter by Roduner. To reiterate briefly, the technique involves the measurement of the time dependent count rate of decay positrons emitted by muons undergoing Larmor precession in an applied transverse field. This count rate is given by

$$F(t) = N_o \times \left[BG + e^{-t/\tau_\mu} \left(1 + A(t)\right) \right] \qquad (1)$$

where N_o is a normalisation constant, BG is a time independent background and

$$A(t) = A_\perp G_\perp(t) \cos\left(\omega t + \phi\right) \qquad (2)$$

$A_\perp$ is the initial asymmetry of the muon decay, and $G_\perp(t)$ represents the muon spin depolarisation function which, in the case of a Type II superconductor, results from the distribution of local fields in the vortex state. As discussed in the extensive review by Aegerter and Lee in this volume, the form of $G_\perp(t)$, or more precisely the fourier transform of $A(t)$, can provide unique and detailed insights into flux distribution and hence into the nature of the flux line lattice, vortex configurations, flux lattice melting and flux pinning. However, there are many situations in which only the second moment of the distribution of internal fields, rather than the detailed shape of that distribution, is of interest. In such cases it is generally adequate to replace $G_\perp(t)$ by a simple Gaussian depolarisation function of the form

$$G_\perp(t) = \exp(-\sigma^2 t^2) \qquad (3)$$

which, in turn, implies a simple Gaussian distribution of internal fields with a second moment of

$$\overline{\Delta B^2} = \frac{2\sigma^2}{\gamma_\mu^2} \qquad (4)$$

where γ_μ is the gyromagnetic ratio of the muon. Several experimental studies and numerical simulations have shown this Gaussian approximation to be appropriate, particularly for orientationally averaged polycrystalline samples and in situations in which convolution with other independent sources of broadening, such as demagnetising fields and random pinning obtain [4,5]. Moreover, the approximation is found to provide a reasonable estimate of the second moment of the field distribution even though the distribution itself might not be precisely Gaussian in form.

The second moment of the internal field distribution in a Type II superconductor, is a function of the penetration depth, λ, the coherence length, ξ, and the upper critical field B_{C2}. From the modified London equation [6]

$$\sqrt{\overline{\Delta B^2}} = B_o \sqrt{\sum_{h,k} \frac{\exp(-\xi^2 q_{h,k}^2)}{\left(1 + q_{h,k}^2 \lambda^2 / (1-b)\right)^2}} \qquad (5)$$

B_o is the mean internal field, $b = B_o / B_{C2}$, and the sum is over all non-zero reciprocal lattice vectors, $q_{h,k}$ of the flux line lattice. In the London limit, for which $\xi \rightarrow 0$, and in situations in which the applied field is well above the lower critical field B_{C1}, such that $\lambda\, q_{h,k} \gg 1$, an evaluation of the sum in equation (5) over an hexagonal lattice gives the much simplified form:

$$\sqrt{\overline{\Delta B^2}} = \frac{\sqrt{0.00371}\,\Phi_o}{\lambda^2} \qquad (6)$$

where Φ_0(=2.07x10^{-15} Wb) is the flux quantum. There is thus an extremely simple numerical relationship between the muon depolarisation rate, σ, and the superconducting penetration depth λ, namely

$$\sigma = \frac{75780}{\lambda^2} \qquad (7)$$

where σ is measured in μs^{-1} and λ is measured in nm.

3. The Uemura classification scheme

The superconducting penetration depth, λ, is related directly to two of the principal parameters of the electronic ground state of a material, namely the effective mass of the electron, m^*, and the carrier density, n_s, The general London formula for the zero temperature limit of the penetration depth, $\lambda(0)$ for an isotropic superconductor gives

$$\lambda(0) = \left[\frac{m^*/m_e}{4\pi n_s r_e} \left(1 + \frac{\xi}{l_e} \right) \right]^{1/2} \qquad (8)$$

where n_s is the superconducting electron density, r_e (=2.82x10^{-15}m) is the classical radius of the electron, l_e is the electron mean free path, and ξ is the superconducting coherence length. ξ/l_e defines the dirty limit correction. Correspondingly we can see from equations (7) and (8) that, within the clean limit, ie for ξ/l_e<<1,

$$\sigma(0) \propto \frac{n_s(0)}{m^*} \qquad (9)$$

The linear dependence of T_C upon $\sigma(0)$ observed by Uemura et al [1-3] therefore implies a direct correlation between T_C and $n_s(0)/m^*$ Such a linear correlation is not consistent with the conventional weak coupling limit of BCS theory, in which the electron pairing mechanism is phononic in origin and the Debye frequency, ω_D, defines the energy scale of the pairing such that $T_C \propto \hbar\,\omega_D$. Usually the electronic density of states is structureless on the scale of $\hbar\,\omega_D$ and so T_C is not expected to be directly related to n_s. However, recognising the quasi-two dimensional character of both the high T_C cuprates and the organic superconductors, and also noting that the Fermi energy, E_F, of a non-interacting 2d electron gas is proportional to n_e/m^*, Uemura et al inferred [2,3] that, for these systems at least, the linear correlation may imply $T_C \propto E_F$. Such a relationship is expected if the energy scale of the electron pairing in the superconducting state is comparable to, or exceeds, E_F [7] The possible correlation between T_C and E_F was further demonstrated by considering the variation of the superconducting transition temperature with the effective Fermi temperature, $T_F = E_F/k_B$. For the quasi-2d systems T_F may be estimated directly from the muon depolarisation rate $\sigma(0)$ via the relation

$$k_B T_F = (\hbar^2 \pi) n_{s2d} \big/ m^* \qquad (10)$$

n_{s2d} is the carrier concentration within the superconducting planes calculated from the volume carrier density using $n_s d$, where d is the interplanar spacing. For a 3d system, however, the Fermi temperature is given by

$$k_B T_F = (\hbar^2/2)(3\pi^2)^{2/3} n_s{}^{2/3} \big/ m^* \qquad (11)$$

To determine T_F the measured muon depolarisation rate must therefore be coupled with, for example, the Sommerfeld constant, γ,

$$\gamma = \left(\frac{\pi}{3}\right)^{2/3} \frac{k_B^2 m^* n_e^{1/3}}{\hbar^2} \qquad (12)$$

where n_e is the carrier density. Assuming that n_s at T=0 is equivalent to n_e above T_C we may combine equations (11) and (12) to obtain $k_B T_F \propto \sigma(0)^{3/4} \gamma^{-1/4}$.

Using this parameterisation Uemura et al [2,3] were able to confirm a close correlation between T_C and T_F. The cuprate, heavy fermion, organic, fullerene and Chevrel phase superconductors all follow a similar linear trend with 1/100< T_C/ T_F <1/10, in contrast to the conventional BCS superconductors (Nb, Sn, Al etc) for which T_C/ T_F <1/1000. The "Uemura plot" of log(T_C) against log(T_F), shown in a stylised form in figure 1, thus appears to discriminate dramatically between the "exotic" and "conventional" superconductors. Indeed, on the basis of the Uemura plot it is tempting to place all of the "exotic" superconductors in a single "class" which is quite distinct from the class of conventional BCS superconductors.

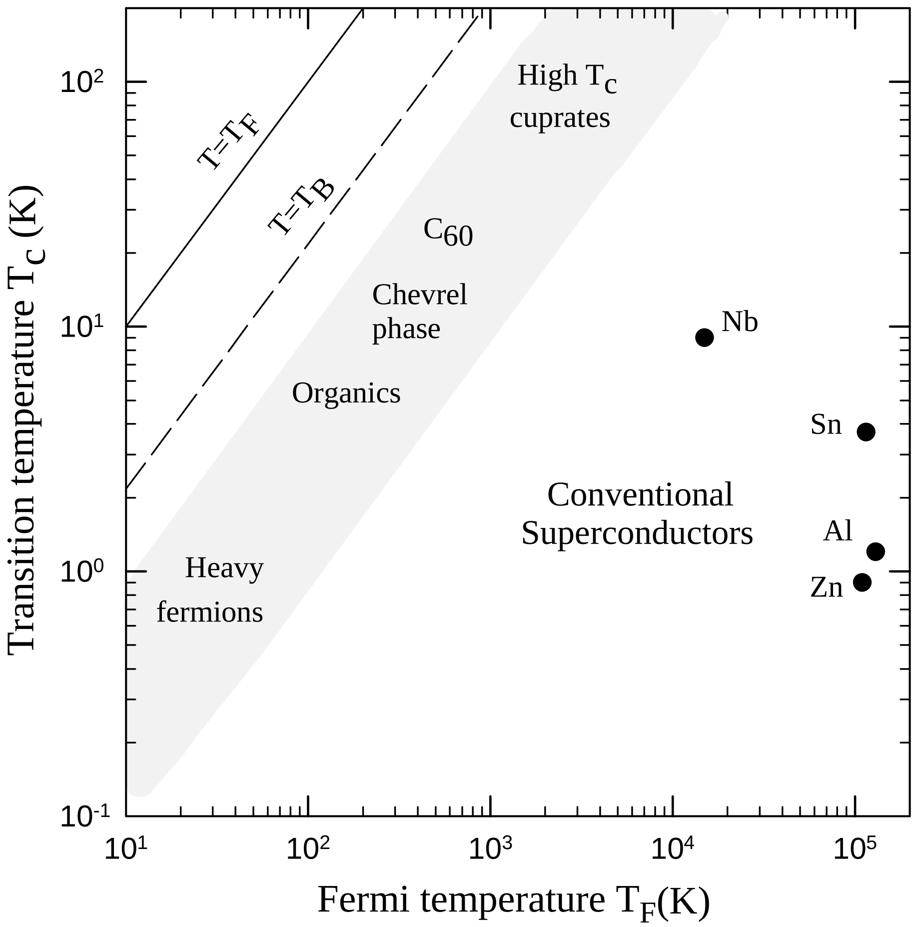

Figure 1: A schematic representation of the "Uemura plot" of superconducting transition temperature T_C against effective Fermi temperature T_F. The "exotic" superconductors fall within a common band for which

$1/100<T_C/T_F<1/10$, indicated by the shaded region in the figure. The dashed line correspond to the Bose-Einstein condensation temperature, T_B, calculated according to equation (13).

The Uemura plot has been taken as an indication that the strongly coupled "exotic" superconductors may, in a thermodynamic sense, be close to Bose-Einstein condensation. The condensation temperature of an ideal boson gas is defined only by n_s and m^*, and is independent of the scale of the pairing interaction, providing that $\hbar\omega_B >> kT_B$ [8] The BE condensation temperature, T_B, represented graphically by the dashed line in the Uemura plot of Figure 1, has been estimated using the expression for an ideal 3d boson gas, ie

$$k_B T_B = (1.04\hbar^2) n_B^{2/3} / m_B \qquad (13)$$

together with a boson density of $n_B = n_s/2$ and boson mass of $m_B=2m^*$. (Although there can be no Bose-Einstein condensation in an perfect 2d system this value of T_B nevertheless provides an estimate of the maximum condensation temperature for the quasi-2d systems discussed here). Intriguingly, all the exotic superconductors are found to have values of T_C/T_B in the range 1/3 to 1/30, thereby emphasising the proximity of these systems to BE-like condensation.

On the basis of these observations it is tempting to suggest that the condensation mechanism in the various exotic superconductors may share a common origin. Indeed, recent calculations within the self consistent renormalisation (SCR) theory of spin fluctuations have suggested that the same antiferromagnetic spin fluctuation mechanism may be responsible for superconductivity in the high T_C cuprates, heavy fermion systems and 2d organic superconductors [9]. Within the SCR theory the energy scale of the pairing mechanism is determined predominantly by the energy width of the dynamic spin fluctuations, T_O. Moreover a linear dependence of T_C upon T_O is derived. Interestingly, the ratio T_C/T_O is of the same order as the ratio T_C/T_B obtained from the Uemura plot, suggesting that energetically T_O and T_B are closely similar. The real space local pairing of superconducting carriers necessary for a BE-like condensation could therefore be mediated by such spin fluctuations.

To summarise, the Uemura formalism has provided a classification scheme which not only discriminates effectively between conventional BCS superconductors and strongly coupled exotic, and perhaps BE-like, superconductors, but also highlights the fundamental similarities between a rather diverse group of exotic superconductors.

4. Borocarbide and hexaboride superconductors

The quaternary borocarbide superconductors have attracted immense interest since their discovery in early 1993 [10-12] . This interest stems in part from their extremely high superconducting transition temperatures (T_C= 23K in the case of Y-Pd-B-C) and in part from the intriguing interplay between the superconducting ground state and the complex magnetic order associated with the 4f ions in the RNi_2B_2C family. These features, together with a layered, tetragonal and highly anisotropic crystal structure not dissimilar to that of the cuprates [13], have fuelled speculation that the borocarbide family may fall within the class of exotic superconductors. However, most experimental and theoretical studies indicate that the borocarbides are more appropriately classified as conventional, phonon mediated BCS superconductors. For example, band structure calculations suggest an essentially isotropic 3d electronic structure and associate the relatively high transition temperatures with a van Hove-like peak in the density of states at the Fermi energy [14]. Experimental evidence for this peak has been provided by studies of the effect of partial 3d transition metal substitution for Ni in YNi_2B_2C [15, 16]. Within the rigid band model such substitution is viewed as shifting the Fermi energy away from the peak of the density of states, thereby reducing T_C. Nevertheless controversy persists: antiferromagnetic spin fluctuations have been invoked to explain the unusual temperature dependence of the B^{11} spin lattice relaxation and Knight shift in YNi_2B_2C and $LuNi_2B_2C$ [17, 18], and, more recently, the presence of superconductivity itself in $LuNi_2B_2C$ [9].

In light of the continuing debate regarding the classification of the borocarbide superconductors we feel it is opportune to extend our earlier μSR studies of the penetration depth in the parent YNi_2B_2C compound [19] with further μSR measurements on $Y(Ni_{1-x}Co_x)_2B_2C$. In this way the correlation between T_C and T_F for the borocarbides can be mapped and interpreted within the Uemura scheme.

As part of the present μSR study we have also chosen to investigate the cubic hexaboride superconductor YB_6 for which no penetration depth measurements exist. There have never been any suggestions this compound is other than a conventional BCS superconductor. It is generally believed that the relatively high transition temperature of 7.1K is a result of strong coupling of the electrons to the Einstein-like modes of the Y ion situated in a cage of B_6 octahedra [20, 21]. However recent crystallographic studies have revealed that the structure of $ThPd_xB_{6-2x}$, a 21K superconductor thought to be related to the borocarbides, is a simple derivative of that of the hexaborides [22]. Consequently YB_6 may also reveal some similarities to the borocarbides family of superconductors.

5. Experimental techniques

All transverse field muon spin rotation spectra were collected using the MuSR spectrometer at the ISIS pulsed muon and neutron facility at the Rutherford Appleton Laboratory, Oxfordshire [23]. At ISIS the pulsed muon beam has a repetition rate of 20ms, and each muon pulse has a width of approximately 70ns. This intrinsic pulse structure provides an appropriate time base with which to time-stamp the detected positrons resulting from the muon decay with the arrival of the pulse defining t=0. The pulsed muon technique has the advantage that although several hundred muons may arrive in the sample within each pulse, coincidence circuits are not required and, moreover the time independent background (BG of equation 1) is essentially zero. However convolution of the finite muon pulse width with the sinusoidal time dependence of the positron count rate results in a marked decrease of the effective asymmetry $A_{\perp}$ with increasing muon precession frequency. At ISIS the range of observable precession frequencies is therefore restricted to somewhat less than 9MHz, and correspondingly applied transverse fields of less than 65mT must be used. Fortunately, such fields are adequate for the experiments we report here.

The $Y(Ni_{1-x}Co_x)_2B_2C$ samples with x=0.05 and x=0.10 were prepared by melting together stoichiometric quantities of the spectrographically pure constituent elements in an argon arc furnace. The resulting ingots were coarsely powdered producing plate like grains. X-ray diffraction confirmed that the resulting material was single phase with the modified $ThCr_2Si_2$ structure (space group I4/mmm) shown in Figure 2a. Low dc field magnetisation and ac susceptibility measurements gave superconducting transition temperatures of 8.6K and 6.2K for $Y(Ni_{0.95}Co_{0.05})_2B_2C$ and $Y(Ni_{0.90}Co_{0.10})_2B_2C$ respectively.

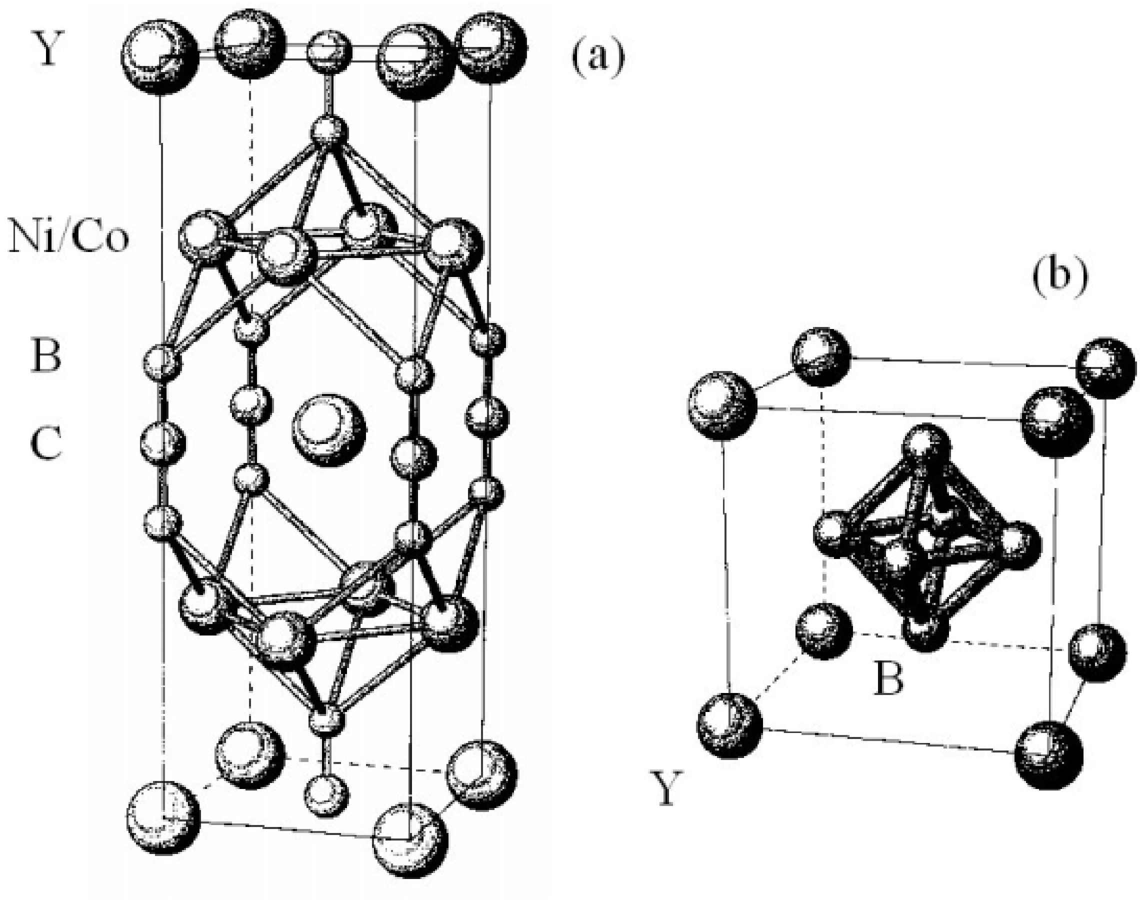

Figure 2 The crystallographic structure of (a) $Y(Ni_{1-x}Co_x)_2B_2C$ and (b) YB_6

The YB_6 powder sample was obtained directly from Aldrich Chemicals. X-ray diffraction revealed a two phase structure. Refinement of the diffraction pattern indicated that the primary phase was YB_6, with the CaB_6 structure (space group Pm3m) shown in Figure 2b. The second phase, which amounted to 30% by volume of the sample, was identified as non-superconducting YB_4. Magnetisation and susceptibility measurements confirmed a superconducting transition temperature of 7.1K for the primary YB_6 phase, in close agreement with published values [21, 24].

The μSR samples consisted of powdered material bonded with epoxy resin to form discs of 25mm in diameter and 3mm thick. The resin constitutes less than 4% by weight of the sample. The sample discs were then mounted on high purity aluminium sample holders masked with Fe_2O_3: muons implanted in haematite depolarise too rapidly to contribute an unwanted background signal over the time regime of interest. Temperatures down to 1.5K were achieved using a top-loading He cryostat. All measurements were taken on warming after first field cooling the sample to base temperature in the appropriate transverse magnetic field.

7. Experimental Results

Figure 3 shows typical μSR spectra collected from the YB_6 sample, in this case at 10K, 4.4K and 1.4K in a transverse field of 40mT. A single lightly Gaussian-damped precession signal provided an excellent fit to the precession signal above the superconducting transition temperature. However below T_C it has proved necessary to introduce a second Gaussian-damped component. The first component is identified with those muons sensing the distribution of internal fields in the mixed state of the superconducting YB_6 matrix, whilst the second is associated with an effective background arising from muons which have stopped in the non-superconducting YB_4 impurity phase. This assignation, and the assumption of Gaussian depolarisation, has been confirmed by fourier transform of the μSR spectra using maximum entropy techniques shown as an inset to figure 3(c).

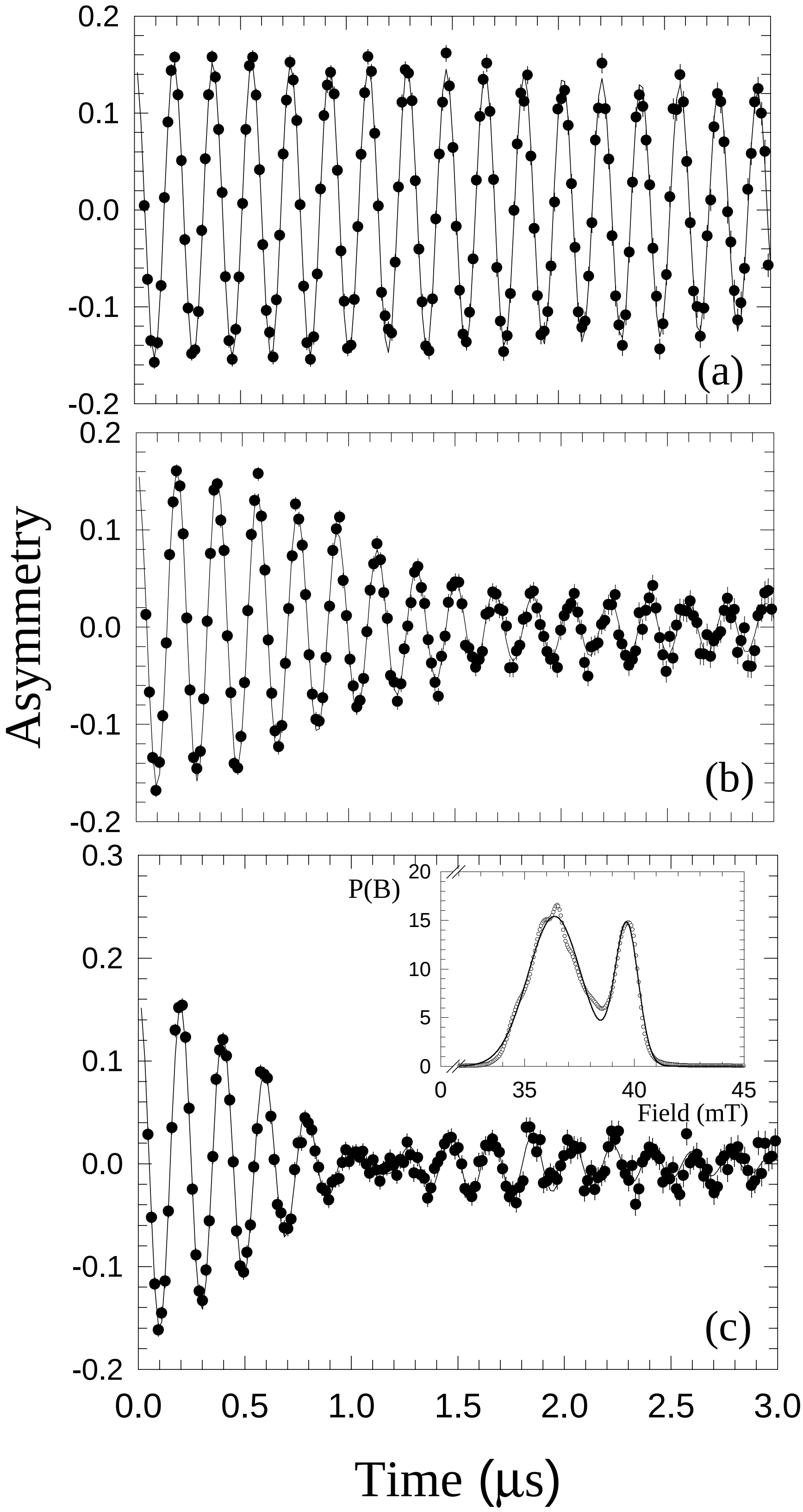

Figure 3 Muon spin rotation spectra obtained from YB_6 in a field of 40mT at a temperature of (a) 10K, in the normal state, and below the superconducting transition at (b) 4.4K and (c) 1.4K. The solid lines represent fits to the data as described in the text. The inset in (b) shows a maximum entropy fourier transform of the 1.4K spectrum. The solid line has been obtained from a fit of

two Gaussian internal field distributions. The first, at 36mT arises from the superconducting YB_6 phase, while the second, narrower, line is due to the substantial background contribution from YB_4 impurities.

For YB_6 both the penetration depth, λ, and the coherence length ξ were obtained directly from the applied magnetic field dependence of the muon spin depolarisation rate, σ, at 1.4K. The field dependence of σ, suitably corrected for the background depolarisation arising from nuclear dipole moments, is shown in figure 4. It can be seen that the modified London expression of equation (5) provides an excellent description of $\sigma(B)$. From the fit of equation (5) to the data we obtain λ=192nm and ξ=33nm.

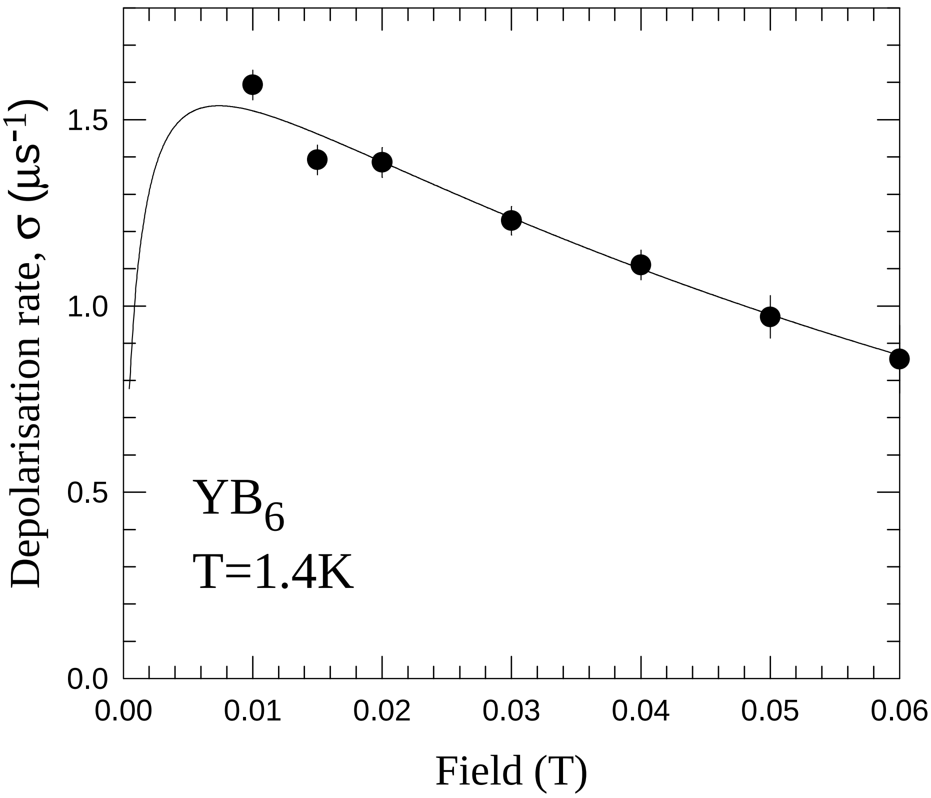

Figure 4 The field dependence of the muon depolarisation rate in YB_6 at 1.4K. The solid line is a fit of the modified London equation (equation 5) to the data, from which a penetration depth, λ, of 192nm and a coherence length, ξ, of 33nm is obtained

The value of λ determined at 1.4K can safely be assumed to represent $\lambda(0)$, as illustrated in figure 5 where the temperature dependence of σ, measured in fields of 15mT and 40mT is shown. The temperature dependence of σ in both applied fields closely follows the form

$$\sigma(T) = \sigma(0)\left[1-\left(\frac{T}{T_C}\right)^N\right] \qquad (14)$$

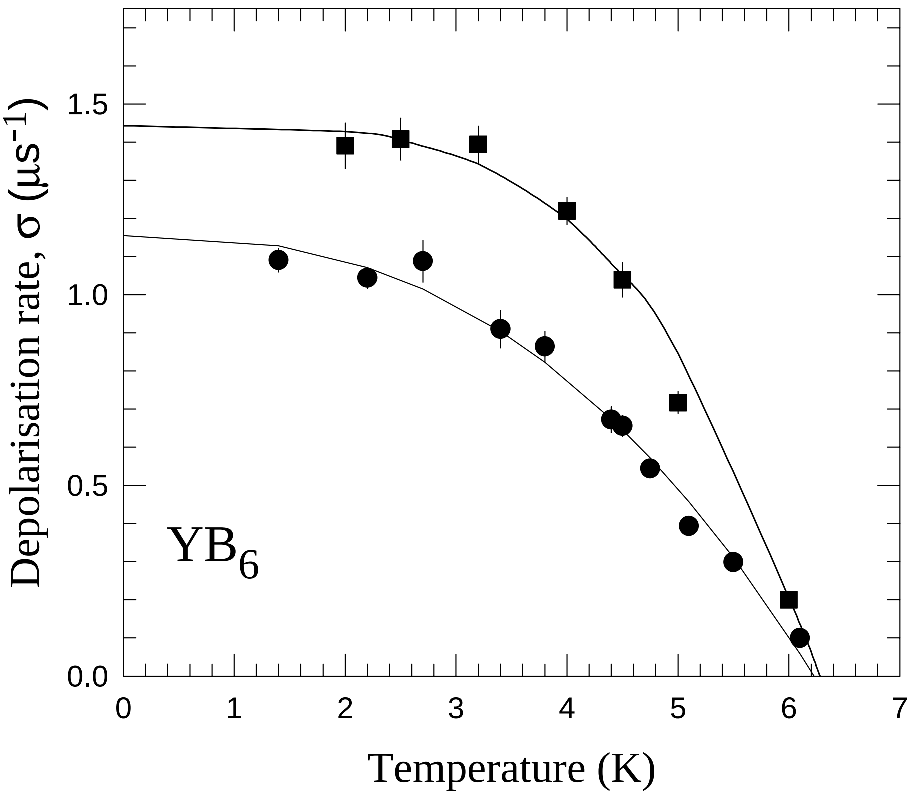

Figure 5 The temperature dependence of the muon depolarisation rate in YB_6 in applied magnetic fields of (■)15mT and (●) 40mT. The solid lines are fits of the *N*-fluid model of equation 14 to the data.

A least squares fit of equation (14) to the data collected in B=15mT yields N=4.0(1), which is fully consistent with the conventional two-fluid model. By 40mT, however, N has decreased to 2.4(1) suggesting a field-induced decrease of the pair binding strength. For both fields a transition temperature of T_C=6.2K was determined from the least squares fit. The suppression of T_C relative to that obtained on the same sample from magnetisation measurements is a consequence of field cooling the sample in fields substantially greater than B_{C1}.

Figure 4 has clearly shown the importance of choosing the appropriate applied field in which to determine σ, and hence a precise estimate of $\lambda(0)$. However, our previous μSR measurements [19] have shown that the coherence length of YNi_2B_2C is relatively short (ξ=8nm). The penetration depth determined from the value of $\sigma(0)$ measured in 40mT closely approximates to that obtained from a fit of equation (5) to the measured field dependence of σ. We have therefore restricted our μSR measurements on $Y(Ni_{0.95}Co_{0.05})_2B_2C$ and $Y(Ni_{0.90}Co_{0.10})_2B_2C$ to a single transverse field of 40mT. In figure 6 we show the temperature dependence of σ for the $Y(Ni_{0.95}Co_{0.05})_2B_2C$ and $Y(Ni_{0.90}Co_{0.10})_2B_2C$ samples in this applied field. The temperature dependence is again well modelled by equation (14), with N=3.1(1) and N=2.0(1) being obtained for the $Y(Ni_{0.95}Co_{0.05})_2B_2C$ and $Y(Ni_{0.90}Co_{0.10})_2B_2C$ samples respectively. These values of N are somewhat lower than the two fluid value of N=4 found for the parent YNi_2B_2C compound and indicate a substantial decrease in the pair binding strength with increasing Co concentration. Substitution of σ, extrapolated to T=0, in equation (7) gives $\lambda(0)$=150nm for $Y(Ni_{0.95}Co_{0.05})_2B_2C$ and $\lambda(0)$=250nm for $Y(Ni_{0.90}Co_{0.10})_2B_2C$, which compare with $\lambda(0)$=103nm obtained from similar μSR measurements on YNi_2B_2C [19].

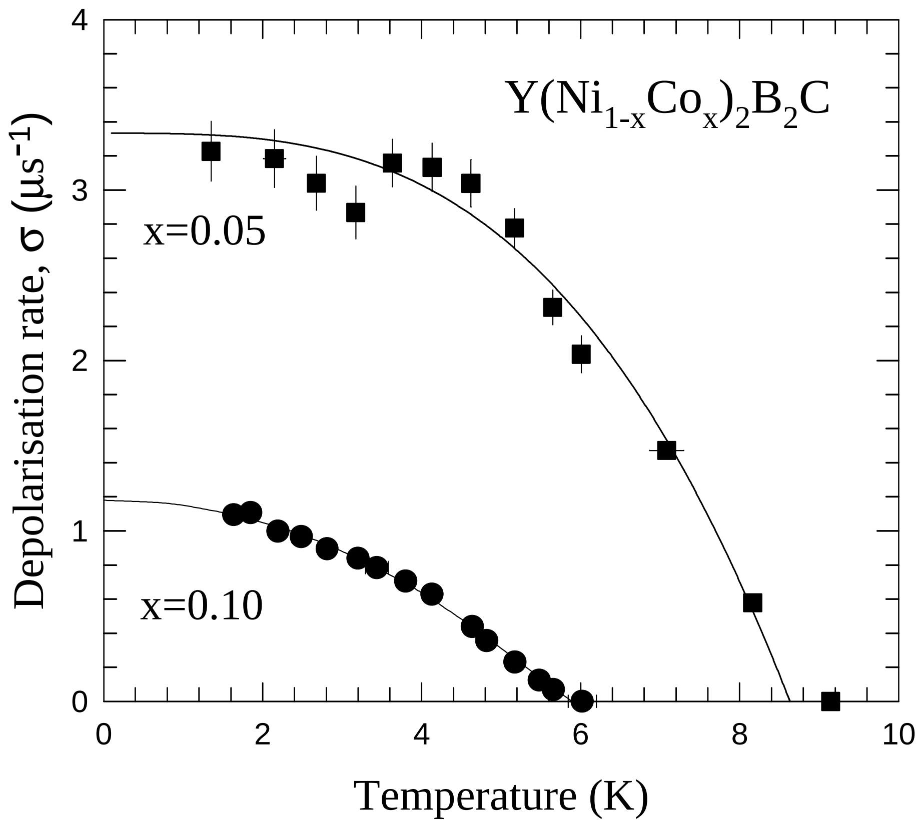

Figure 6 The temperature dependence of the muon depolarisation rate in $Y(Ni_{0.95}Co_{0.05})_2B_2C$ (■) and $Y(Ni_{0.90}Co_{0.10})_2B_2C$ (●) in an applied magnetic fields of 40mT. The solid lines are fits of the *N*-fluid model of equation 14 to the data.

8. Discussion

Using the values of the penetration depth obtained from our μSR measurements on YB_6, $Y(Ni_{0.95}Co_{0.05})_2B_2C$ and $Y(Ni_{0.90}Co_{0.10})_2B_2C$ together with published thermodynamic data we can extract the values for the superconducting carrier density and the effective mass of the carriers shown in Table I, where the corresponding values for YNi_2B_2C are also listed. It should be noted that we have, as yet, no reliable estimate for the dirty limit correction for YB_6. However, on the basis of published resistivity measurements [21,25] we have some justification for assuming that YB_6 is within the clean limit. For $Y(Ni_{0.95}Co_{0.05})_2B_2C$ and $Y(Ni_{0.90}Co_{0.10})_2B_2C$ resistivity measurements indicate a similar dirty limit correction *(ξ/l_e = 0.16)* to that found for the parent YNi_2B_2C compound [19].

	T_C (K)	$\lambda(0)$ (nm)	n_s ($x10^{28}$ m^{-3})	m*/m	T_F (K)	T_C/T_F
YB_6	7.1	192	0.24	3.1	2433	1/343
YNi_2B_2C	15	103	2.9	9.4	4200	1/280
$Y(Ni_{0.95}Co_{0.05})_2B_2C$	8.6	150	1.4	11.3	2180	1/250
$Y(Ni_{0.90}Co_{0.10})_2B_2C$	6.2	250	0.6	10.8	1238	1/200

Table 1: A summary of the superconducting ground state parameters of the YB_6 and $Y(Ni_{1-x}Co_x)_2B_2C$ compounds obtained from μSR and thermodynamic studies. The values for YNi_2B_2C have been taken from reference [19]

The reported value of γ for YB_6 is 2.8mJ.mol^{-1}.K^{-2} [24] Correspondingly, using equations (8) and (12) we obtain *$m^*/m=3.1$* and n_S= 2.4x10^{27} m^{-3}. The mass enhancement of the carriers in YB_6 is considerably lower than that of YNi_2B_2C compound [19]. The carrier density is also relatively low, representing only 20% of the single conduction electron per Y ion anticipated for the trivalent rare earth hexaborides. The associated Fermi temperature of YB_6 estimated from equation (11) is 2433K, yielding a ratio for T_C/T_F of 1/343. Within the Uemura classification scheme YB_6, like YNi_2B_2C, therefore lies extremely close to the boundary separating exotic from conventional superconducting systems. This perhaps provides the first indication that superconductivity in YB_6 may not be entirely conventional

Heat capacity measurements on the $Y(Ni_{1-x}Co_x)_2B_2C$ system have provided Sommerfeld constants of 15.2mJ.mol^{-1}K^{-2} and 12mJ.mol^{-1}K^{-2} for compounds with x=0.05 and x=0.10 respectively [16]. Combining these values with the measured penetration depths we estimate an effective carrier mass enhancement of *m^*/m*=11.3 for $Y(Ni_{0.95}Co_{0.05})_2B_2C$ and *m^*/m*=10.8 for $Y(Ni_{0.90}Co_{0.10})_2B_2C$. These values are consistent with that of 9.4 obtained previously for YNi_2B_2C [19]. The carrier density, n_s, on the other hand, decreases dramatically with increasing Co concentration, falling from $2.9 \times 10^{28} m^{-3}$ for YNi_2B_2C, to $1.4 \times 10^{28} m^{-3}$ for $Y(Ni_{0.95}Co_{0.05})_2B_2C$ and $0.6 \times 10^{28} m^{-3}$ for $Y(Ni_{0.90}Co_{0.10})_2B_2C$. The associated values for T_C/T_F are 1/280, 1/250 and 1/200 respectively. While, at first sight, these values appear to preclude $Y(Ni_{0.90}Co_{0.10})_2B_2C$ from the unified class of exotic superconductors, the compounds cannot readily be classed as conventional superconductors. T_C/T_F is still rather high, and the almost linear relationship between T_C and T_F as Co concentration is varied may be an indication of an underlying exotic pairing mechanism, such as the proposed antiferromagnetic spin fluctuations [9], which leads to BE-like condensation.

Although general consensus has suggested that YB_6 and the $Y(Ni_{1-x}Co_x)_2B_2C$ compounds are conventional BCS superconductors, our μSR results indicate that neither system can be readily classified as either “conventional” or “exotic”, at least within the Uemura scheme. Instead they appear to sit uneasily at the border between the two regimes, as can be seen in Figure 7.

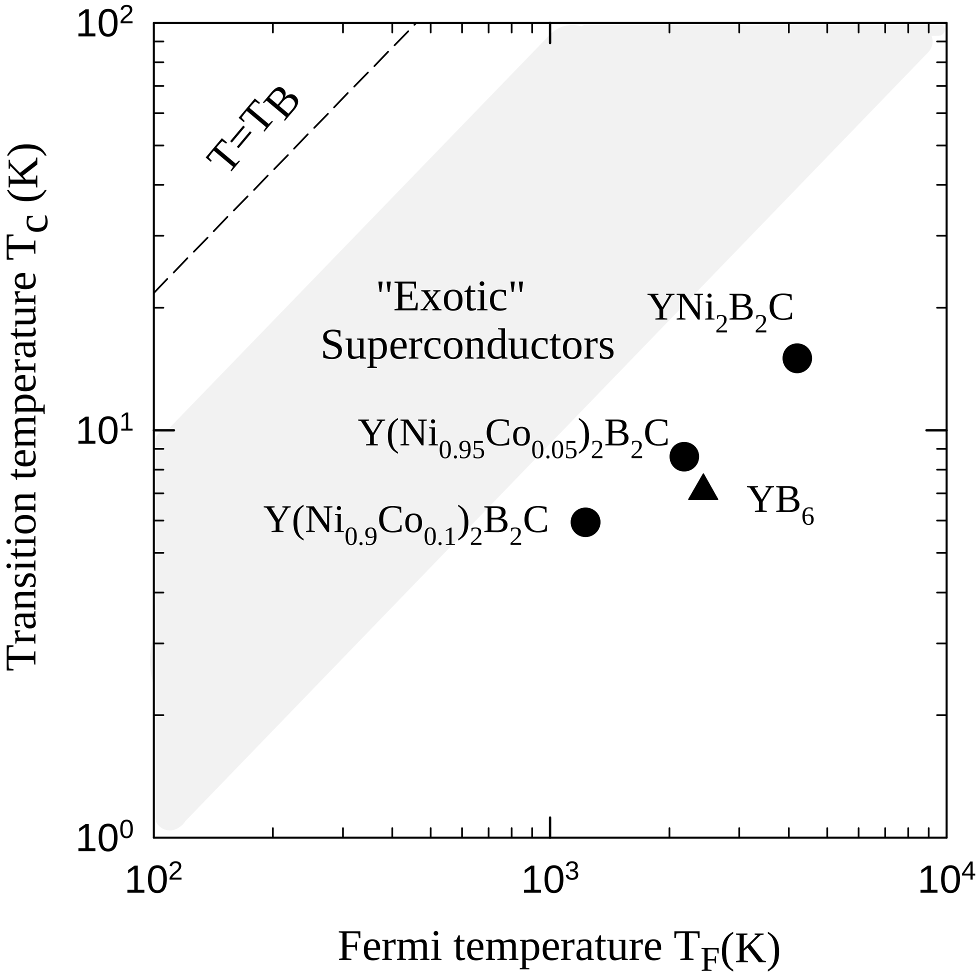

Figure 7 The results of the μSR experiments on YB_6, YNi_2B_2C (from [19]), $Y(Ni_{0.95}Co_{0.05})_2B_2C$ and $Y(Ni_{0.90}Co_{0.10})_2B_2C$ summarised on the Uemura plot of T_C vs T_F. The proximity of all four compounds to the so-called "exotic" superconductors is evident. Of particular note is the approximately linear scaling followed by the $Y(Ni_{1-x}Co_x)_2B_2C$ compounds.

Acknowledgements

It is a pleasure to acknowledge our collaboration with C Aegerter, Z-P Han, S H Kilcoyne, S L Lee and C A Scott in the course of this work. We are grateful for financial support from the UK Engineering and Physical Sciences Research Council. ADH acknowledges receipt of an EPSRC Research Studentship.

References

[1] Y J Uemura, G M Loke, B J Sternlieb, J H Brewer, J F Carolan, W N Hardy, R Kadono,

J R Kempton, R F Kiefl, S R Kreitzman, P Mulhern, T M Riseman, D Ll Williams,

B X Yang, S Uchida, H Takagi, J Gopalkrishnan, A W Sleight, M A Subramanian,

C L Chien, M Z Cieplak, Gang Xiao, V Y Lee, B W Statt, C E Stronach, W J Kossler and

X H Yu, Phys Rev Let 62 (1989) 2317

[2] Y J Uemura, L P Le, G M Luke, B J Sternlieb, W D Wu, J H Brewer, T M Riseman,

C L Seaman, M B Maple, M Ishikawa, D G Hinks, J D Jorgensen, G Saito and

H Yamochi, Phys Rev Let 66 (1991) 2665

[3] Y J Uemura, Physica C 185-189 (1991) 733

[4] B Pumpin, H Keller, W Kundig, W Odermatt, I M Savic, J W Schneider, H Simmler and

P Zimmermann, Phys Rev B 42 (1990) 8019

[5] M Weber, A Mato, F N Gygax, A Schenck, H Maletta, V N Duginov, V G Grebinnik,

A B Lazarev, V G Olshevsky, V Yu Pomjakushin, S N Shilov, V A Zhukov, B F Kirillov,

A V Pirogov, A N Ponomarev, V G Storchak, S Kapusta and J Bock,

Phys Rev B 48 (1993) 13022

[6] E H Brandt, Phys Rev B 37 (1988) 2349

[7] V J Emery and G Reiter, Phys Rev B 38 (1988) 4547

[8] R Mincus, J Ranninger and S Rabaszkiewicz, Rev Mod Phys 62 (1990) 113

[9] S Nakamura, T Moriya and K Ueda, J Phys Soc Japan 65 (1996) 4026

[10] C Mazumdar, R Nagarajan, C Godart, L C Gupta, M Latroche, S K Dhar,

C Levy-Clement, B D Padalia and R Vijayaghavan Solid State Commun, 87 (1993) 413

[11] R Nagarajan, C Mazumdar, Z Hossain, S K Dhar, K V Gopolakrisnan, L C Gupta, C Godart, B D Padalia and R Vijayaghavan, Phys Rev Lett 72 (1994) 274

[12] R J Cava, H Takagi, B Batlogg, H W Zandbergen, J J Krajewski, W F Peck Jr, R B van Dover, R J Felder, T Siegrist, K Mizuhashi, J O Lee, H Eisaki, S A Carter and S Uchida, Nature (London) 367 (1994) 146

[13] T Siegrist, H W Zandbergen, R J Cava, J J Krajewski and W F Peck Jr, Nature 367 (1994) 254

[14] J I Lee, T S Zhao, I G Kim, B I Min and S J Youn, Phys Rev B 50 (1994) 4030

[15] A K Gangopadhyay, A J Scheutz and J S Schilling, Physica C 246 (1995) 317

[16] C C Hoellwarth, P Klavins and R N Shelton, Phys Rev B 53 (1996) 2579

[17] T Kohara, T Oda, K Ueda, Y Yamada, A Mahajan, K Elankumaran, Z Hossian, L C Gupta, N Nagarajan, R Vijayaraghavan and C Mazumdar Phys Rev B 51 (1995) 3985

[18] K Ikushima, J Kikuchi, H Yasuoka, R J Cava, H Takagi, J J Krajewski and W F Peck Jr, J Phys Soc Japan 63 (1994) 2878

[19] R Cywinski, Z P Han, R I Bewley, R Cubitt, M T Wylie, E M Forgan, S L Lee, M Warden and S H Kilcoyne Physica C 233 (1994) 273

[20] G Schell, H Winter, H Rietschel and F Gomf, Phys Rev B 25 (1982) 1589

[21] S Kunii, Y Kasuya, K Kadowaki, M Date and S B Woods, Solid State Commun 52 (1984) 659

[22] H W Zanderbergen, E J van Zwet, J Jansen, J L Sarrao, M B Maple, Z Fisk and R J Cava,

Phil Mag Lett 71 (1995) 131

[23] G H Eaton, Z Phys C: Particles and Fields 56 (1992) S232

[24] B T Matthias, T H Geballe, K Andres, E Corenzwit, G W Hull, and J P Maita, Science 159 (1968) 530

[25] T Tanaka, T Akahane, E Bannai, S Kawai. N Tsuda and Y Ishizawa, J Phys C: Solid State Phys 9 (1976) 1235

Figure Captions